GOVT. DOC.

Y 3. N 21/5:6/1930

NACA TN 1930

NATIONAL ADVISORY COMMITTEE FOR AERONAUTICS

TECHNICAL NOTE 1930

AN ANALYSIS OF THE EFFECT OF LIFT-DRAG RATIO AND STALLING SPEED ON LANDING-FLARE CHARACTERISTICS

By J. Calvin Lovell and Stanley Lipson

Langley Aeronautical Laboratory
Langley Air Force Base, Va.

Washington
September 1949

STATE LIBRARY

SEP 9 1949

BUSINESS, SCIENCE
& TECHNOLOGY DEP'T.

NATIONAL ADVISORY COMMITTEE FOR AERONAUTICS

TECHNICAL NOTE 1930

AN ANALYSIS OF THE EFFECT OF LIFT-DRAG RATIO AND STALLING SPEED ON LANDING-FLARE CHARACTERISTICS

By J. Calvin Lovell and Stanley Lipson

SUMMARY

Calculations of the landing-flare paths of a series of hypothetical airplanes having systematically varying characteristics have been made to provide information concerning the effects of maximum lift coefficient, wing loading, and lift-drag ratio on the landing-flare characteristics. Charts are presented which indicate the effects of current design trends on landing-flare velocity and distance requirements and which permit the rapid estimation of the flare characteristics of any airplane having an approximately constant lift-drag ratio during the landing flare. A method for predicting the landing-flare characteristics of an airplane having a variable lift-drag ratio during the flare is given in an appendix. The application of the analysis is demonstrated by the determination of the effects of high-lift devices on landing characteristics of three transonic wing configurations.

Airplanes landing at low lift-drag ratios will have relatively high sinking speeds at the start of the flare and at an altitude of 50 feet, even if the stalling speeds are relatively low. Airplanes which have relatively low lift-drag ratios and high stalling speeds will require power-off landing flares to start at relatively high altitudes. These results indicate that power-off landings of some airplanes designed specifically from high-speed considerations may not be feasible at conventional airports. Airplanes having high stalling speeds will require relatively large horizontal distances for either power-on or power-off landing flares.

INTRODUCTION

The increased application of airfoils and wing plan forms designed specifically from high-speed considerations has resulted in airplanes having relatively low maximum lift coefficients, low lift-drag ratios, and high wing loadings. These design trends increase the stalling speed and gliding angle of airplanes; hence, an adverse effect on the landing maneuver is indicated. In order to provide information concerning this effect, the landing flares of a series of hypothetical

airplanes have been calculated on the basis of an assumed flare plan. The flare plan assumed is based primarily on reference 1, in which information permitting calculation of the flare characteristics of an airplane was obtained from flight tests. The results of calculations for airplanes having constant lift-drag ratio during the flare are plotted in chart form.

In addition, since the drag increase, often resulting from deflection of high-lift devices, may adversely affect the power-off landing of airplanes which already have low lift-drag ratios, the effect of the high-lift devices of three transonic wing configurations on landing-flare characteristics was determined.

SYMBOLS

C_L	lift coefficient (L/qS)
$C_{L_{max}}$	maximum lift coefficient
L	lift, pounds
D	drag, pounds
L/D	lift-drag ratio
W	weight of airplane, pounds
S	wing area, square feet
W/S	wing loading, pounds per square foot
q	free-stream dynamic pressure, pounds per square foot $\left(\frac{\rho V_f^2}{2}\right)$
ρ	mass density of air, slugs per cubic foot
V_f	velocity along the flight path, feet per second
V_v	vertical velocity or sinking speed, feet per second
γ	flight-path angle, degrees $\left(\sin^{-1}\frac{V_v}{V_f}\right)$

V_s	stalling speed, feet per second $\left(\sqrt{\frac{2(W/S)}{\rho C_{L_{max}}}}\right)$
$\sqrt{\frac{W/S}{C_{L_{max}}}}$	factor proportional to V_s; at sea level numerically equals $\frac{V_s}{29.0}$
s_h	horizontal distance, feet
s_v	vertical distance, feet
a_n	acceleration normal to flight path, g units
$a_{n_{max}}$	maximum normal acceleration
a_f	deceleration along the flight path, feet per second per second
g	acceleration due to gravity, 32.2 feet per second per second
t	time measured from end of flare, seconds
Subscripts:	
a	approach condition
b	condition at $0.85C_{L_{max}}$

LANDING-FLARE CALCULATIONS

The landing maneuver begins with a steady-state approach to a position at a relatively low altitude and off the end of the runway from which the landing flare is executed. The flare is the leveling-off phase of the landing maneuver, during which the vertical velocity and altitude are reduced to zero. The accomplishment of an acceptable landing depends primarily on the pilot's ability to execute the landing flare so that contact with the runway is made at a low vertical velocity and at a reasonably low forward speed.

The landing approach, being a steady-state glide, is defined when the speed and equivalent value of L/D of the airplane (equivalent because D may include the effect of thrust) are known.

The landing flare depends primarily on the aerodynamic characteristics of the airplane and the flare plan used by the pilot. In order to calculate the effects of only the aerodynamic characteristics on the flare characteristics, a general landing-flare plan must be assumed.

It is realized that in a practical case a pilot cannot follow any predetermined landing plan closely and that the general flare plan assumed for the present analysis may not be entirely realistic over a wide range of lift-drag ratio. In addition, ground effect has been neglected in order to simplify the calculations. Since the primary purpose of this paper is to present a comparison of flare characteristics and illustrate general trends, it is believed that these assumptions do not significantly affect the results.

The assumptions concerning excess speed and lift-coefficient variation in the flare, based primarily on reference 1, which define the general flare plan assumed for the present analysis are as follows:

The speed of an airplane at the start of the landing flare must be sufficiently above the stalling speed to provide the acceleration necessary to curve the flight path so that the runway is approached tangentially. The degree of curvature or abruptness of the flare depends on the magnitude of the excess-speed ratio $\frac{V_f - V_s}{V_s}$. A start-of-flare (initial) excess-speed ratio of 0.25 was used in reference 1 for the airplane studied. Preliminary calculations showed that the initial-excess-speed ratio required for completion of a flare increases as the value of L/D decreases and that a value of 0.25 is too low to permit completion of flares at low values of L/D. In order to provide a common basis for calculation and comparison of flares of airplanes having a wide range of values of L/D, a fixed end-of-flare (final) excess-speed ratio for all values of L/D was assumed. A value of 0.15 was chosen, based on landing records at moderate values of L/D.

In order to facilitate calculation the flare is considered to consist of three phases:

Phase I is the transition period required to increase the value of C_L from the value in the approach to the maximum value reached in the flare. This increase in C_L is assumed to be effected in 2 seconds by a sinusoidal increase in normal acceleration.

Phase II is the period of deceleration at the highest lift coefficient reached in the flare, which is assumed to be $0.85C_{L_{max}}$. The duration of phase II depends on the vertical velocity at the start of the phase and the rate at which it is being decreased. In the flare calculations, phase II continues until the vertical velocity is decreased to the value which is to be lost in phase III.

Phase III is the transition period during which the value of C_L is decreased from $0.85C_{L_{max}}$ to the value for level flight at the end of the flare where V_f equals $1.15V_s$. The change in C_L is assumed to occur in 1 second as the result of a sinusoidal decrease in normal acceleration. At the end of phase III the vertical velocity is zero and the flare is complete. This general flare plan permits calculation by a step-by-step method of the landing-flare characteristics of an airplane having a known stalling speed and L/D polar. An exact solution is precluded by the inability to write equations expressing the variation of the accelerations with time in all phases of the flare. The step-by-step calculations are simplified by a solution starting from the end of the flare and proceeding consecutively through phases III, II, and I because all the end-of-flare conditions are known, whereas the initial excess speed is unknown. This method of calculation is given in detail in the appendix.

RESULTS AND DISCUSSION

The general landing-flare plan has been used as a basis for the calculation of the landing-flare paths of a series of hypothetical airplanes having a range of lift-drag ratio from 2.5 to 20.0 and a range of stalling speed from 60 miles per hour to 475 miles per hour at sea level. A constant value of L/D during the flare was assumed for each airplane. The results of these calculations have been plotted in chart form to show the effect of current design trends on landing-flare velocity and distance requirements and to permit prediction of the landing performance of proposed airplanes.

In addition, the power-off landing-flare paths of three transonic wing configurations have been calculated, and the high-lift devices of each airplane have been evaluated.

Landing-Flare Charts

The assumption of a constant lift-drag ratio during the flare of a particular airplane permits the compilation in chart form of the results of the landing-flare calculations. The assumption of a constant value of L/D is feasible for most straight-wing airplanes in the landing condition as indicated by figure 1, which gives the variation of lift-drag ratio with lift coefficient obtained from wind-tunnel tests, for some representative airplanes. For some airplanes, however, such as those having extreme sweepback, the value of L/D often varies considerably during the flare as shown in figure 1.

In this case, the charts do not apply and a separate flare calculation must be made.

General trends.- The excess-speed ratio required at the start of the flare for completion of the general flare plan is given in figure 2. The curve shown is the locus of the required initial-excess-speed ratios determined by the step-by-step calculations for the ranges of L/D and stalling speed used, and it indicates an increasing excess-speed ratio with decreasing L/D which is independent of stalling speed. Unfortunately, extensive flight data are not available for comparison with the calculated initial-excess-speed-ratio curve. However, pilot observations during glides and landings of several airplanes having lift-drag ratios between 4 and 5 (power-off landings recently made at the Langley Laboratory of fighter-type airplanes having propellers) and the initial-excess-speed ratios given for the airplane of reference 1 $\left(\frac{L}{D} = 7.9\right)$ indicate that the trend of the curve and order of magnitude of the required initial-excess-speed ratios are realistic. As the value of L/D decreases below about 4, the indicated initial-excess-speed ratio increases rapidly to values appreciably higher than those generally associated with present-day airplanes. A presently proposed high-speed airplane having a triangular wing (airplane A of fig. 1) indicates a power-off initial-excess-speed requirement of $0.57V_s$, which corresponds to a speed loss during the flare of $0.42V_s$. At relatively high values of L/D the loss in speed during the flare is small and, accordingly, the excess speed required at the start of the flare is low. For a flare at a value of L/D of 10 the decrease in speed during the flare is $0.05V_s$, and at a value of L/D of 20 the decrease is $0.01V_s$.

Figure 3 shows the effect of lift-drag ratio and stalling speed $\left(V_s \propto \sqrt{\frac{W/S}{C_{L_{max}}}}\right)$ on the flight speed and sinking speed at the start of the flare. At a constant value of L/D the flight speed increases in proportion to the stalling speed, because the loss in speed during the flare is a constant percentage of stalling speed. Correspondingly, at a constant value of L/D the sinking speed at the start of the flare, which is proportional to the approach speed, also varies directly with the stalling speed. For a given stalling speed, the sinking speed increases as the value of L/D decreases because of the steepening of the glide-path angle and the increasing excess-speed requirements.

The maximum normal acceleration and the time duration of the calculated flare paths are given in figures 4 and 5, respectively. Figure 4 indicates that the maximum normal acceleration is primarily

dependent on the lift-drag ratio, although at a low value of L/D stalling speed has some effect. Since the maximum normal acceleration, at a given stalling speed, is proportional to the excess-speed ratio, the maximum normal acceleration increases as the value of L/D decreases. The calculated landing flares have a minimum-time requirement of 3 seconds because the flare plan assumes a 2-second phase I and a 1-second phase III. At a constant value of L/D, the increase in time required is approximately proportional to the increase in stalling speed (fig. 5) and, at a given stalling speed, the time required decreases as the value of L/D increases.

The horizontal-distance requirements for the landing flare are shown in figures 6 and 7, in which the limiting lines (dashed) are vertical-velocity contours of 10 and 75 feet per second. The horizontal distance required at a constant value of L/D increases at an increasing rate with stalling speed (see fig. 6) because both the flight speed during the landing flare and the time required for the flare increase with stalling speed. At a constant stalling speed, changes in the lift-drag ratio effect relatively small changes in horizontal distance because, as shown in figures 3 and 5, variations in the lift-drag ratio effect only small changes in flight velocity and landing-flare time. The horizontal distance required from an altitude of 50 feet to the end of the flare (fig. 7) is also primarily dependent on stalling speed. At a given stalling speed, however, this distance increases somewhat as the value of L/D increases.

The total vertical distance required for the flare, or altitude at which the flare must be started, is shown in figure 8 to increase as stalling speed increases and the value of L/D decreases.

These results indicate that the combination of high stalling speed and low lift-drag ratios encountered in many proposed high-speed airplanes will result in relatively high power-off gliding speeds and sinking speeds at the start of the flare and, compared with conventional airplanes, will require greater vertical and horizontal distances for completion of the flare. The convergence of the vertical velocity and distance contours of figures 3 and 8, respectively, indicates that at low values of L/D an incremental change in stalling speed effects a relatively large change in the rate of descent and the altitude at which the flare must be started.

Vertical velocity-altitude relationship.- The vertical velocity to be encountered during the landing of an airplane is an important consideration affecting the pilot's ability to execute successfully the landing flare. High vertical speeds in the approach complicate the judging of the altitude at which the flare should be started, and high vertical speeds in the final stages of the landing flare increase the difficulty of simultaneously decreasing vertical velocity and

altitude to zero. Because the significance of vertical velocity depends on the corresponding altitude, the variation of vertical velocity with altitude is considered an important factor. For the airplane of reference 1, sinking speeds above 25 feet per second at the start of the flare (approx. 50-ft altitude) could not be consistently handled with safety and accuracy. Figures 9(a) and 9(b) show the sinking-speed variation with altitude for airplanes having constant values of L/D of 4 and 7.5, respectively, and various start-of-flare sinking speeds (corresponding to different stalling speeds). The plots indicate that at a constant lift-drag ratio the vertical velocity remaining at an altitude of 50 feet is virtually independent of the initial vertical velocity. At a lift-drag ratio of 4 for various stalling speeds, start-of-flare sinking speeds varying from 35 to 75 feet per second are reduced to a range from 33 to about 38 feet per second at an altitude of 50 feet, and likewise at a value of L/D of 7.5, start-of-flare sinking speeds from 25 to 45 feet per second are reduced to a range from 24.5 to 28.5 feet per second at an altitude of 50 feet. Although the vertical velocity at an altitude of 50 feet is relatively independent of stalling speed, it increases with decreasing value of L/D. The effect of lift-drag ratio on the vertical velocity at an altitude of 50 feet for a representative stalling speed is shown in figure 10. The start-of-flare vertical velocities have been included in the figure for comparison. Although the vertical velocity lost during the initial phases of the landing flare increases as the lift-drag ratio decreases, the vertical velocity remaining at an altitude of 50 feet also continues to increase with decreasing value of L/D. The sinking speed at 50 feet increases from 21 feet per second at a value of L/D of 10 to 43 feet per second at a value of L/D of 3. These results indicate that airplanes landing at low values of L/D and having high sinking speeds in the approach will also have relatively high sinking speeds at an altitude of 50 feet, even though the stalling speeds may be low.

Prediction of flare characteristics.- The landing-flare charts can be used to predict the flare characteristics of an airplane having a small-percentage variation in lift-drag ratio during the flare. If the value of L/D is not approximately constant the charts do not apply, and a separate flare calculation by the method described in the appendix is necessary.

In the case of a power-off landing flare of an airplane having given values of $C_{L_{max}}$, W/S, and L/D, the flare velocities, distance, and other flare characteristics are obtained directly from figures 3 to 8. The power-on flare characteristics can be predicted by considering that the thrust of the airplane is used to adjust the approach value of L/D to the value which will give the desired start-of-flare vertical velocity. For the chosen value of V_v and the

known values of W/S and $C_{L_{max}}$, figure 3 gives the corresponding value of L/D, which in conjunction with the value of W/S and $C_{L_{max}}$ permits the determination of the other flare characteristics from figures 4 to 8. The increment between this value of L/D and the power-off value of L/D at the same lift coefficient is indicative of the thrust required to obtain the desired sinking speed.

Power-Off Evaluation of High-Lift Devices

An analysis by the method presented herein of the power-off landing-flare characteristics of three transonic airplane wings indicates relative merits of high-lift devices not apparent from wind-tunnel data. Since each of the wings considered had no fuselage, canopy, or landing gear, the results obtained are to be used only on a comparative basis. The lift coefficients given are not trimmed lift coefficients. The percentage variation in L/D during the flare for some of these configurations was appreciable, in which case the charts were inapplicable and individual flare calculations were made. The details of the configurations, for which wing loadings of 40 pounds per square foot were assumed, and a summary of the results obtained are given in table I.

Wing swept back 37°.- A low-speed investigation of a wing with the leading edge swept back 37° had been previously conducted to determine the effect of split flaps and double slotted flaps on the aerodynamic characteristics. The basic wing had a value of $C_{L_{max}}$ of 1.27 and an approach value of L/D of 14.2, which give a start-of-flare flight speed of 195 feet per second at a sinking speed of 14 feet per second. Deflecting the split flaps increased the value of $C_{L_{max}}$ to 1.65 and decreased the value of L/D in the approach to 6.3. The net effect is a slight reduction in the start-of-flare flight speed and an increase in sinking speed to 30 feet per second, which required starting the flare 40 feet higher. The use of the double slotted flap increased the value of $C_{L_{max}}$ to 2.32 at an approach value of L/D of 8.0 and resulted in a desirable 45-foot-per-second decrease in approach flight speed with only a 4-foot-per-second increase in sinking speed and an appreciable reduction in the horizontal distance required for the flare (see table I). These results demonstrate the importance of considering the changes in lift-drag ratio often resulting from the use of high-lift devices.

Wing swept back 48°.- The advantages of leading-edge flaps on a wing with the leading edge swept back 48° are indicated by prediction of the landing-flare characteristics. The basic wing had start-of-flare sinking and gliding speeds of 37 feet per second and 263 feet per second, respectively, a horizontal-distance requirement of 1250 feet, and a starting altitude of 90 feet. The deflection of leading-edge

flaps increased $C_{L_{max}}$ only about 0.2 but effected a sizeable increase in lift-drag ratio which reduced the start-of-flare sinking speed to almost one-half the former value and, also, substantially decreased the approach speed and the distance requirements. Trailing-edge flaps installed on this wing gave slightly larger increases in maximum lift coefficient, but corresponding decreases in the value of L/D nullify any improvement in flare characteristics.

Triangular wing.- The landing flare of a triangular wing of equilateral plan form indicates poor landing characteristics. The basic wing had a $C_{L_{max}}$ of 1.08 and an approach value of L/D of 5.4 which give start-of-flare sinking and gliding speeds of 47 feet per second and 264 feet per second, respectively, and vertical- and horizontal-distance requirements of 105 feet and 1080 feet, respectively. Semispan and full-span leading-edge and trailing-edge flaps tested on this wing gave slight increases in $C_{L_{max}}$ and decreases in the approach L/D which effected no appreciable improvement in flare characteristics. Similar undesirable power-off landing characteristics are predicted for the triangular-wing airplane (configuration A of fig. 1 (gear down)), which indicates a start-of-flare sinking speed of 70 feet per second at an altitude of 176 feet and a sinking speed of 43 feet per second at an altitude of 50 feet. The high sinking speeds in the low-altitude stages of the flare could be reduced by the use of a higher initial excess speed and lower lift coefficients during the flare. This method of reducing sinking speed, however, increases the horizontal-distance requirement. These results indicate that power-off landings at conventional airports of some triangular-wing airplanes may not be feasible.

A comparison of the distance requirements of the basic triangular wing with those of a hypothetical wing, having the same value of $C_{L_{max}}$ (1.08) and a constant value of L/D of 5.4 throughout the flare, indicates that a decreasing lift-drag ratio during the flare reduces the distance requirements. If the value of L/D of the triangular wing had remained constant during the landing flare, the vertical and horizontal distances would have been increased to 130 feet and 1250 feet, respectively.

In connection with triangular-wing airplanes, the large attitude change likely to be required in the landing flare because of the low aspect ratio and the low lift-drag ratio is considered a factor that may complicate the landing technique. The landing-flare calculations, by giving the lift coefficients and flight path during the flare, permit determination of the attitude of the airplane. Figure 11 shows the attitude of the triangular wing at three points during a power-off landing flare and, for comparison, the corresponding attitudes during a

power-off flare of a straight-wing airplane (configuration C of fig. 1). The results indicate an attitude change of 18° for the triangular wing, whereas for the straight-wing airplane (configuration C) the variation in attitude is only $9\frac{1}{2}^{\circ}$.

SUMMARY OF RESULTS

The results of calculations to determine the effect of airplane aerodynamic characteristics on landing-flare characteristics are summarized as follows:

1. The excess-speed ratio $\frac{V_f - V_s}{V_s}$ required at the start of the flare increases as the lift-drag ratio of an airplane decreases, and at a lift-drag ratio below about 4, initial-excess-speed ratios increase rapidly above those generally associated with present-day airplanes.

2. For power-off landings of some airplanes designed specifically from high-speed considerations, the changes in lift-drag ratio resulting from deflection of high-lift devices have first-order effects on landing-flare characteristics and may nullify the effect of maximum-lift-coefficient increases. The present analysis provides a basis for determining the combined effect of maximum lift coefficient and lift-drag ratio on landing-flare characteristics.

3. Airplanes landing at low lift-drag ratios will have relatively high sinking speeds at the start of the flare and at an altitude of 50 feet even if the stalling speeds are relatively low. For the landing-flare plan assumed in the present analysis, the magnitude of the vertical velocity at 50 feet is primarily dependent on the lift-drag ratio.

4. Power-off landing flares of airplanes which have relatively low lift-drag ratios and high stalling speeds will be required to start at relatively high altitudes.

5. Results 3 and 4 indicate that power-off landings of some airplanes designed specifically from high-speed considerations may not be feasible at conventional airports.

6. Airplanes having high stalling speeds (low maximum lift coefficient and high wing loading) will require relatively large horizontal distances for either power-on or power-off landing flares.

Langley Aeronautical Laboratory
National Advisory Committee for Aeronautics
Langley Air Force Base, Va., May 11, 1949

APPENDIX

METHOD OF CALCULATING LANDING FLARE

The method of calculating the landing flare of an airplane is described herein. In order to facilitate calculation the flare is considered to consist of three phases as discussed in the section entitled "Landing-Flare Calculations." As an illustration of the computational procedure, the results of step-by-step calculations of the landing flare of airplane A (fig. 1) are given in table II. The step-by-step calculations are begun at the end of the flare and progress consecutively through phases III, II, and I because all of the conditions at the end of the flare are known, whereas the start-of-flare excess speed is unknown. In the discussion which follows, the numerical subscripts will refer to time in seconds measured from the end of the flare.

The variation of normal acceleration with time during the flare is shown in figure 12.

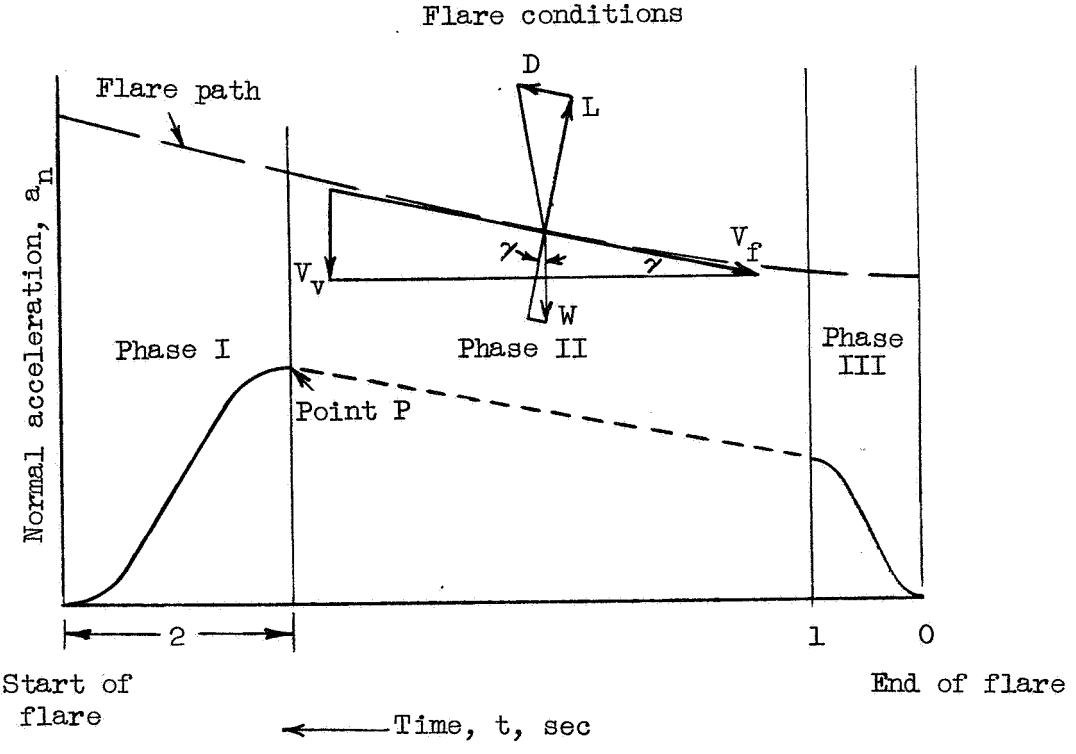

Figure 12.- Variation of normal acceleration with time during landing flare.

The conditions known at the start of the calculations (end of flare) are as follows:

$V_v = 0$
$V_f = 1.15V_s$ feet per second
$a_n = 1.0$
$a_f = 32.2\frac{D}{L}$ feet per second per second (see formula given in section entitled "Phase III")

Phase III

Normal accelerations.- In phase III, the normal acceleration a_n increases sinusoidally from 1.0 at t_0 to the value at $0.85C_{L_{max}}$ at $t_{1.0}$. The value of a_n at $0.85C_{L_{max}}$ can be estimated from figure 13 by use of the average value of L/D corresponding to C_{L_0} and $0.85C_{L_{max}}$. This value of $a_{n_{1.0}}$ is checked when the step-by-step calculations have proceeded to 1 second. If the value of $V_{f_{1.0}}$ and the assumed value of $a_{n_{1.0}}$ do not correspond to $0.85C_{L_{max}}$, a new value of $a_{n_{1.0}}$ is assumed. This is a converging process requiring few estimates.

The formula for a_n during phase III is

$$a_n = \frac{a_{n_{1.0}} - 1}{2}\left[1 + \sin\frac{\pi}{2}(2t - 1)\right] + 1$$

where t represents the time in seconds from the end of the flare.

Vertical velocity.- In the calculation of vertical velocity during the flare, the cosine of the flight-path angle is considered unity. (At the maximum flight-path angle considered in the analysis, $\cos\gamma > 0.99$ during phase III and $\cos\gamma > 0.97$ during phase II. In phase I, when $\cos\gamma$ reaches a minimum value of 0.94, the value of a_n is relatively small; thus, the error in V_v is negligible.) The vertical-velocity increase during any time increment Δt is therefore represented by the area under the normal acceleration-time curve for that increment and is given by the following formula:

$$\Delta V_v = 32.2\,\frac{a_{n_{1.0}} - 1}{2}\int_t^{t+\Delta t}\left[1 + \sin\frac{\pi}{2}(2t - 1)\right]dt$$

The evaluation of this integral for the $\frac{1}{2}$-second time intervals used in the calculation of phase III gives

$$\Delta V_{v_{0.0 \text{ to } 0.5}} = 2.92\left(a_{n_{1.0}} - 1\right)$$

$$\Delta V_{v_{0.5 \text{ to } 1.0}} = 13.18\left(a_{n_{1.0}} - 1\right)$$

The vertical velocity at the end of each time increment equals the velocity at the start of the increment plus the velocity change during the increment.

Vertical distance.- The vertical distance covered is given by the following formula:

$$s_v = 32.2 \frac{a_{n_{1.0}} - 1}{2} \left[\frac{t^2}{2} - \frac{\sin \frac{\pi}{2}(2t - 1)}{\pi^2} - \frac{1}{\pi^2}\right]$$

The evaluation of this formula for phase III gives

$$\Delta s_v = 4.79\left(a_{n_{1.0}} - 1\right)$$

Deceleration along flight path.- Deceleration along the flight path a_f is derived by use of the vector diagram of figure 12:

$$\text{Force in direction of flight} = W \sin \gamma = W \frac{V_v}{V_f}$$

$$\text{Force in drag direction} = \left(\frac{D}{L}\right)L = \left(\frac{D}{L}\right)a_n W \cos \gamma$$

Then,

$$a_f = 32.2\left[\left(\frac{D}{L}\right)a_n \cos \gamma - \frac{V_v}{V_f}\right]$$

In the determination of a_f from this formula at a specific time during phase III, the values of a_n and V_v are known, and the values of V_f, D/L, and $\cos \gamma$ for the previous increment are used. The time increments are chosen small enough to permit this approximation.

Flight velocity.- The flight-velocity increase during a time increment is calculated from the average of the decelerations at the

start and end of the increment. The flight velocity at the end of each time increment equals the velocity at the start of the increment plus the velocity gained during the increment.

Horizontal distance.- The horizontal distance covered during a time increment is calculated from the average of the horizontal velocities at the beginning and at the end of the increment.

C_L and L/D.- The values of C_L and L/D at any time are determined from the corresponding values of V_f, a_n, and $\cos \gamma$. The formula for C_L is

$$C_L = \frac{2a_n \frac{W}{S} \cos \gamma}{\rho V_f^2}$$

Phase II

Phase II is calculated by considering that the values of a_n and a_f are constant over the time increment chosen for one step of the calculations. Since a_n changes substantially in 1/2 second and the acceleration-time history is not predetermined as in phases III and I, $\frac{2}{10}$-second time increments were used in the calculation of phase II. The step-by-step development of phase II is demonstrated by formulas for the first step.

Vertical velocity.- The formula for obtaining the vertical-velocity change during a $\frac{2}{10}$-second time increment is

$$\Delta V_{v_{1.0 \text{ to } 1.2}} = 32.2\left(a_{n_{1.0}} - 1\right)\Delta t$$

The vertical velocity at end of each time increment equals the velocity at start of increment plus the velocity change during the increment; or

$$V_{v_{1.2}} = V_{v_{1.0}} + \Delta V_{v_{1.0 \text{ to } 1.2}}$$

Flight velocity.- The formulas for obtaining the flight-velocity change and the flight velocity at end of each time increment are as follows:

$$\Delta V_{f_{1.0 \text{ to } 1.2}} = a_{f_{1.0}} \Delta t$$

$$V_{f_{1.2}} = V_{f_{1.0}} + \Delta V_{f_{1.0 \text{ to } 1.2}}$$

Normal acceleration.- The value of $a_{n_{1.2}}$ can be calculated when $V_{f_{1.2}}$ is known. At constant C_L, $a_n \approx V_f^2$; thus,

$$a_{n_{1.2}} = \left(\frac{V_{f_{1.2}}}{V_{f_{1.0}}}\right)^2 a_{n_{1.0}}$$

Deceleration along flight path.- The value of $a_{f_{1.2}}$ is calculated by the formula derived in the analysis of phase III; thus,

$$a_{f_{1.2}} = 32.2\left[\left(\frac{D}{L}\right)_{1.2} a_{n_{1.2}} \cos \gamma_{1.2} - \frac{V_{v_{1.2}}}{V_{f_{1.2}}}\right]$$

Vertical distance and horizontal distance.- The vertical and horizontal distances covered in one time increment of phase II are calculated from the average of the vertical and horizontal velocities, respectively, at the beginning and at the end of the increment.

This procedure is continued in $\frac{2}{10}$-second steps until a point is reached from which the execution of phase I will result in start-of-flare conditions that satisfy the requirement of zero deceleration along the flight path; that is, $\frac{V_v}{V_f} = \frac{D}{L} \cos \gamma$. The point at which phase I should be started is determined by trial. If phase I is started too early, the value of a_f at the start of the flare is positive; and if phase I is started too late, the value of a_f is negative. An estimation of the point at which phase I should be started may be obtained as follows: By use of the value of L/D at $0.85C_{L_{max}}$ obtain from figure 2 an approximate value of initial-excess-speed ratio and corresponding approach V_f. Then, use this

value of V_{f_a} to approximate C_{L_a}, $(L/D)_a$, and V_{v_a} (subscript a refers to approach). The vertical velocity at the start of phase I plus the vertical velocity to be gained in phase I (see section that follows) should equal V_{v_a}.

Phase I

Normal acceleration.- In phase I, the normal acceleration a_n decreases sinusoidally from its value at the start of phase I to 1.0 two seconds later. The formula for a_n during phase I is

$$a_n = \frac{a_{n_P} - 1}{2}\left[1 + \sin\frac{\pi}{2}(t' + 1)\right] + 1$$

where subscript P refers to point at which the calculation of phase I is started (see fig. 12) and t' is time from the start of the calculation of phase I.

Vertical velocity.- The vertical-velocity increase during any time increment Δt is given by the following formula:

$$\Delta V_v = 32.2\,\frac{a_{n_P} - 1}{2}\int_{t'}^{t'+\Delta t}\left[1 + \sin\frac{\pi}{2}(t' + 1)\right]dt$$

The evaluation of this integral for $\frac{1}{2}$-second intervals gives

ΔV_v first half-second of phase I = $15.30(a_{n_P} - 1)$

ΔV_v second half-second of phase I = $11.05(a_{n_P} - 1)$

ΔV_v third half-second of phase I = $5.05(a_{n_P} - 1)$

ΔV_v final half-second of phase I = $0.80(a_{n_P} - 1)$

The vertical velocity at the end of each time increment equals the velocity at the start of the increment plus the velocity change during the increment.

Vertical distance.- The vertical distance covered is given by the following formula:

$$s_v = V_{v_p} t' + 32.2 \frac{a_{n_p} - 1}{2} \left[\frac{t'^2}{2} - \frac{4}{\pi^2} \sin \frac{\pi}{2}(t' + 1) + \frac{4}{\pi^2} \right]$$

The evaluation of this formula for phase I gives

$$\Delta s_v = 2V_{v_p} + 45.25\left(a_{n_p} - 1\right)$$

Deceleration along flight path, flight velocity, and horizontal distance.- The deceleration along the flight path, the flight velocity, and the horizontal distance are calculated by the method used in phase III.

REFERENCES

1. Gustafson, F. B., and O'Sullivan, William J., Jr.: The Effect of High Wing Loading on Landing Technique and Distance, with Experimental Data for the B-26 Airplane. NACA ARR L4K07, 1945.

TABLE I.- SUMMARY OF LANDING-FLARE CHARACTERISTICS FOR THREE TRANSONIC WING PLAN FORMS

[Computations based on $\frac{W}{S}$ = 40 lb/sq ft]

Wing plan form	Aspect ratio	Taper ratio	Configuration	$C_{L_{max}}$	$(L/D)_a$	$(L/D)_b$	V_{v_a} (ft/sec)	V_{f_a} (ft/sec)	s_h (ft)	s_v (ft)
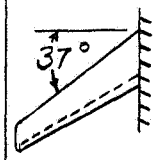	6	0.5	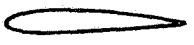	1.27	[1]14.2	12.3	14	195	800	30
			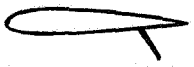	1.65	[1]6.3	6.4	30	180	800	70
			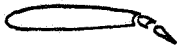	2.32	[1]8.0	6.9	18	150	600	40
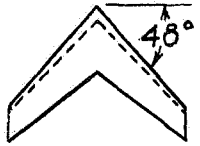	3.5	0.5		0.87	[2]7.1	3.7	37	263	1250	90
			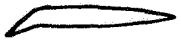	1.09	[2]10.1	6.9	23	216	960	51
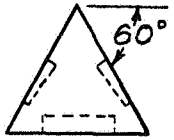	2.3	0	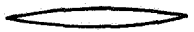	1.08	[2]5.4	2.4	47	264	1080	105
			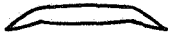	1.20	[2]5.8	2.8	41	240	960	90

[1]Percentage variation of L/D during the flare sufficiently small to permit use of charts.

[2]Percentage variation of L/D during the flare too great to permit use of charts.

TABLE II.- STEP-BY-STEP CALCULATIONS OF THE LANDING FLARE OF AIRPLANE A OF FIGURE 1

$\left[C_{L_{max}} = 0.99, \frac{W}{S} = 40 \text{ lb/sq ft}\right]$

t	C_L	a_n	ΔV_v	V_v	a_f	ΔV_f	V_f	s_v	s_h	L/D	D/L	cos γ
0	0.75	1.00		0	11.9		211.6	0	0	2.7	0.37	1.000
			0.8			6.4						
.50	.81	1.14		.8	13.5		218.0	.1	107.4	2.4	.42	1.000
			3.6			7.5						
1.00	.84	1.27		4.4	16.5		225.5	1.3	218.3	2.3	.43	1.000
			1.7			3.3						
1.20	.84	1.31		6.1	17.3		228.8	2.4	263.7	2.3	.43	1.000
			2.0			3.5						
1.40	.84	1.35		8.1	17.6		232.3	3.8	309.8	2.3	.43	.999
			2.3			3.5						
1.60	.84	1.39		10.4	17.8		235.8	5.7	356.6	2.3	.43	.999
			2.5			3.6						
1.80	.84	1.43		12.9	18.0		239.4	8.0	404.1	2.3	.43	.999
			2.8			3.6						
2.00	.84	1.47		15.7	18.2		243.0	10.9	452.2	2.3	.43	.998
			3.0			3.6						
2.20	.84	1.52		18.7	18.5		246.6	14.3	501.0	2.3	.43	.997
			3.3			3.7						
2.40	.84	1.56		22.0	18.7		250.3	18.4	550.5	2.3	.43	.996
			3.6			3.7						
2.60	.84	1.61		25.6	18.9		254.0	23.2	600.7	2.3	.43	.995
			3.9			3.8						
2.80	.84	1.66		29.5	19.2		257.8	28.7	651.6	2.3	.43	.994
			4.3			3.8						
3.00	.84	1.71		33.8	19.4		261.6	35.0	703.1	2.3	.43	.992
			4.6			3.9						
3.20	.84	1.76		38.4	19.5		265.5	42.2	755.3	2.3	.43	.990
			4.9			3.9						
3.40	.84	1.81		43.3	19.6		269.4	50.4	808.1	2.3	.43	.987
			.5			.4						
3.42	.84	1.82		43.8	19.6		269.8	51.3	813.4	2.3	.43	.987
			12.5			9.0						
3.92	.72	1.70		56.3	16.5		278.8	76.4	947.8	2.8	.36	.980
			9.1			6.3						
4.42	.57	1.41		65.4	8.5		285.1	107.0	1085.3	3.4	.29	.975
			4.1			2.7						
4.92	.44	1.12		69.5	2.4		287.8	140.9	1224.5	3.9	.26	.972
			.7			.7						
5.42	.39	1.00		70.2	.3		288.5	175.9	1364.6	4.0	.25	.972

[1]Based on conditions at $t = 5.42$, $a_f = 0$.

NACA

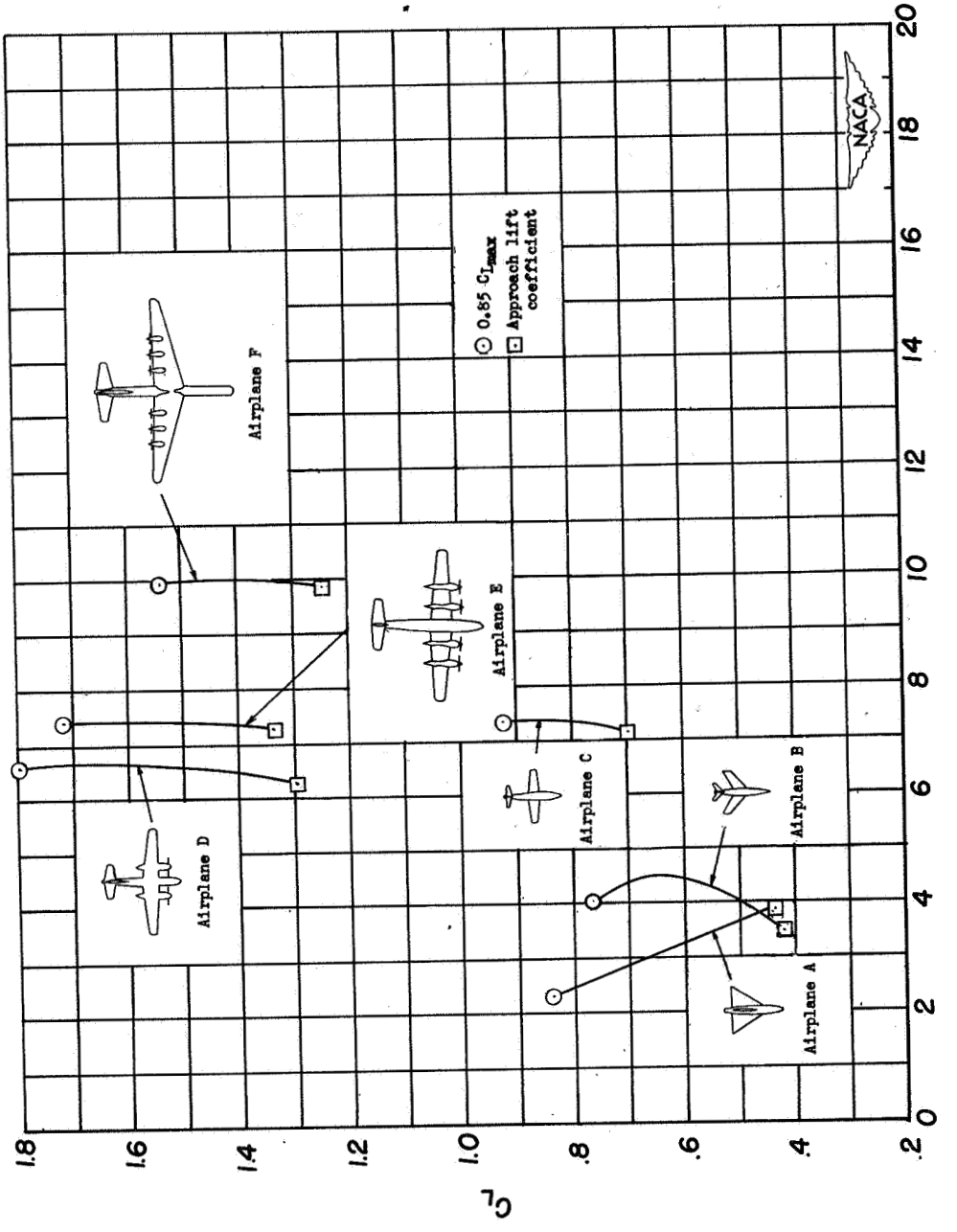

Figure 1.- Variation of C_L with L/D during the landing flare for six representative airplane configurations. Data obtained from wind-tunnel tests for power-off landing condition.

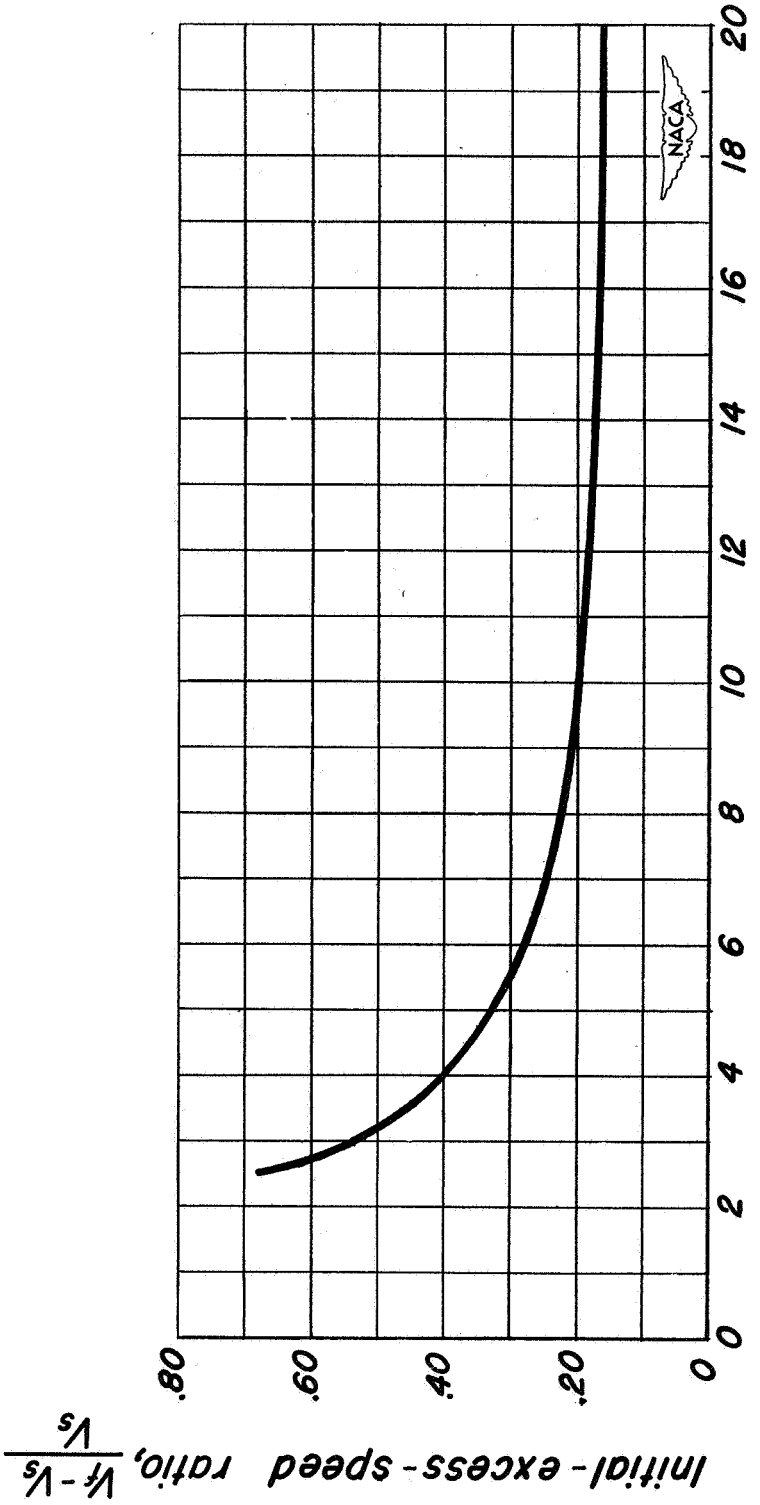

Figure 2.- Start-of-flare excess-speed ratio required for airplanes having a constant value of L/D during the landing flare.

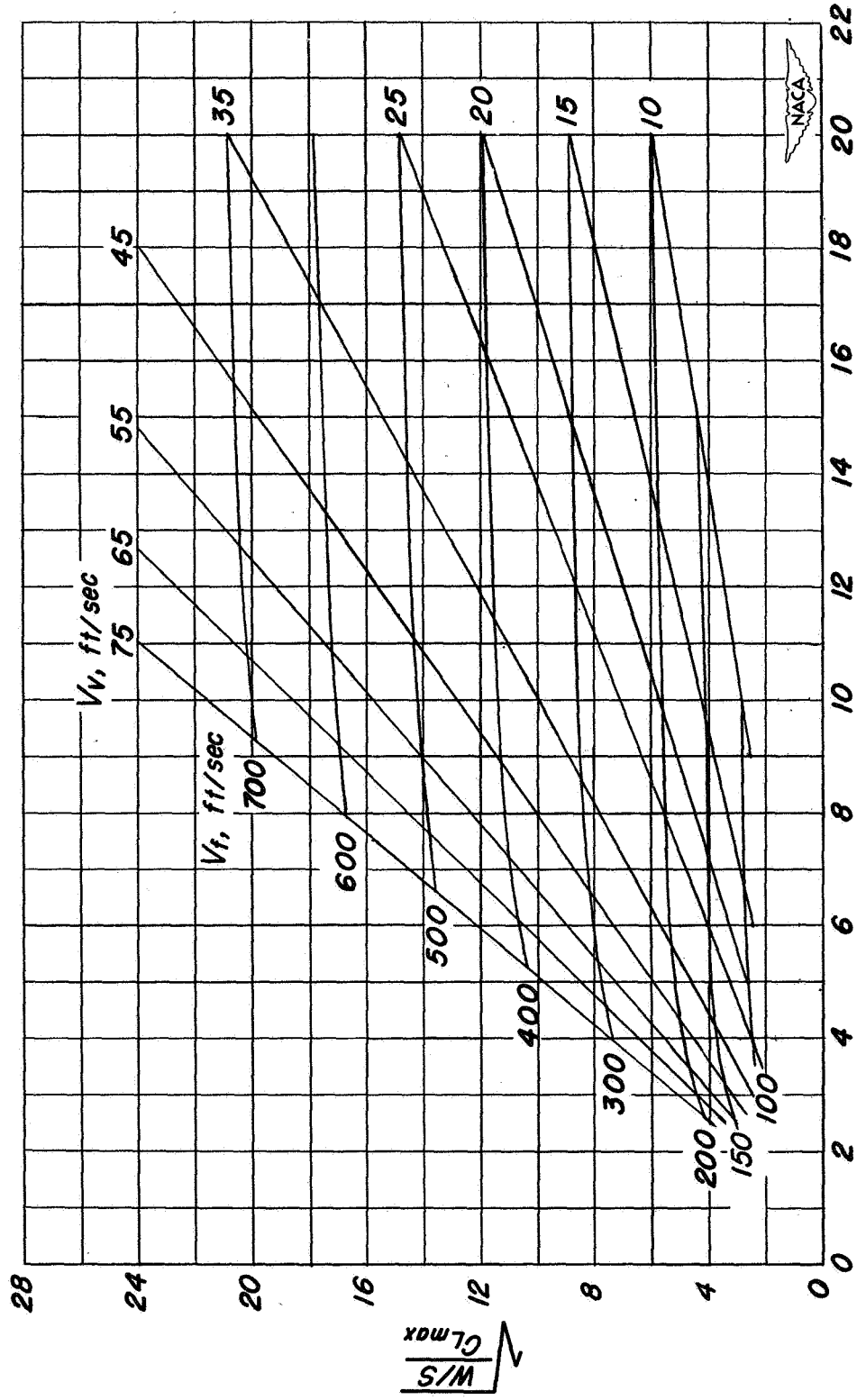

Figure 3.- Variation of the start-of-flare velocities with L/D and $\sqrt{\frac{W/S}{C_{L_{max}}}}$.

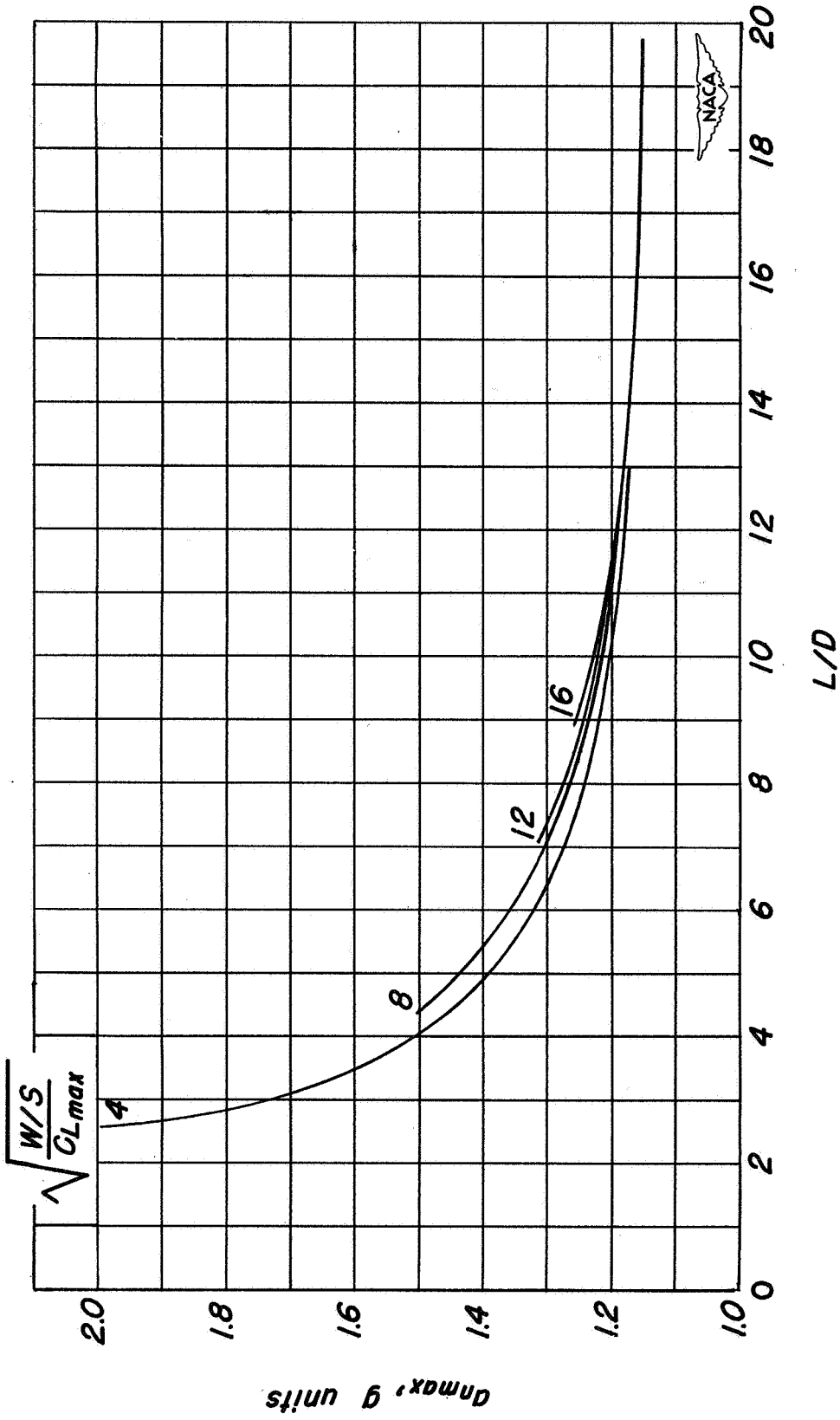

Figure 4.- Variation of the maximum normal acceleration $a_{n_{max}}$ with L/D and $\sqrt{\frac{W/S}{C_{L_{max}}}}$.

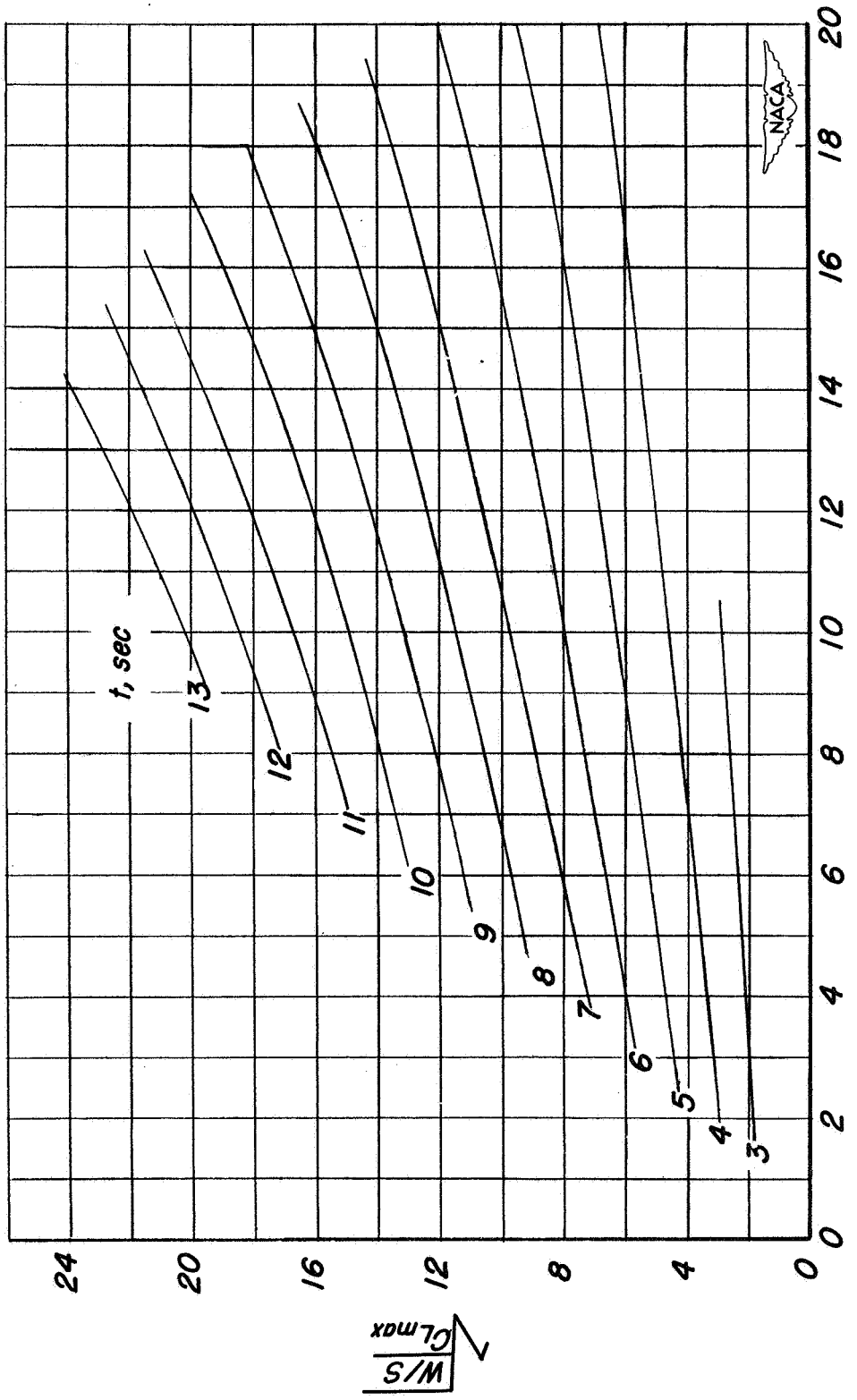

Figure 5.- Variation of time duration of the landing flare with L/D and $\sqrt{W/S}_{C_{L_{max}}}$.

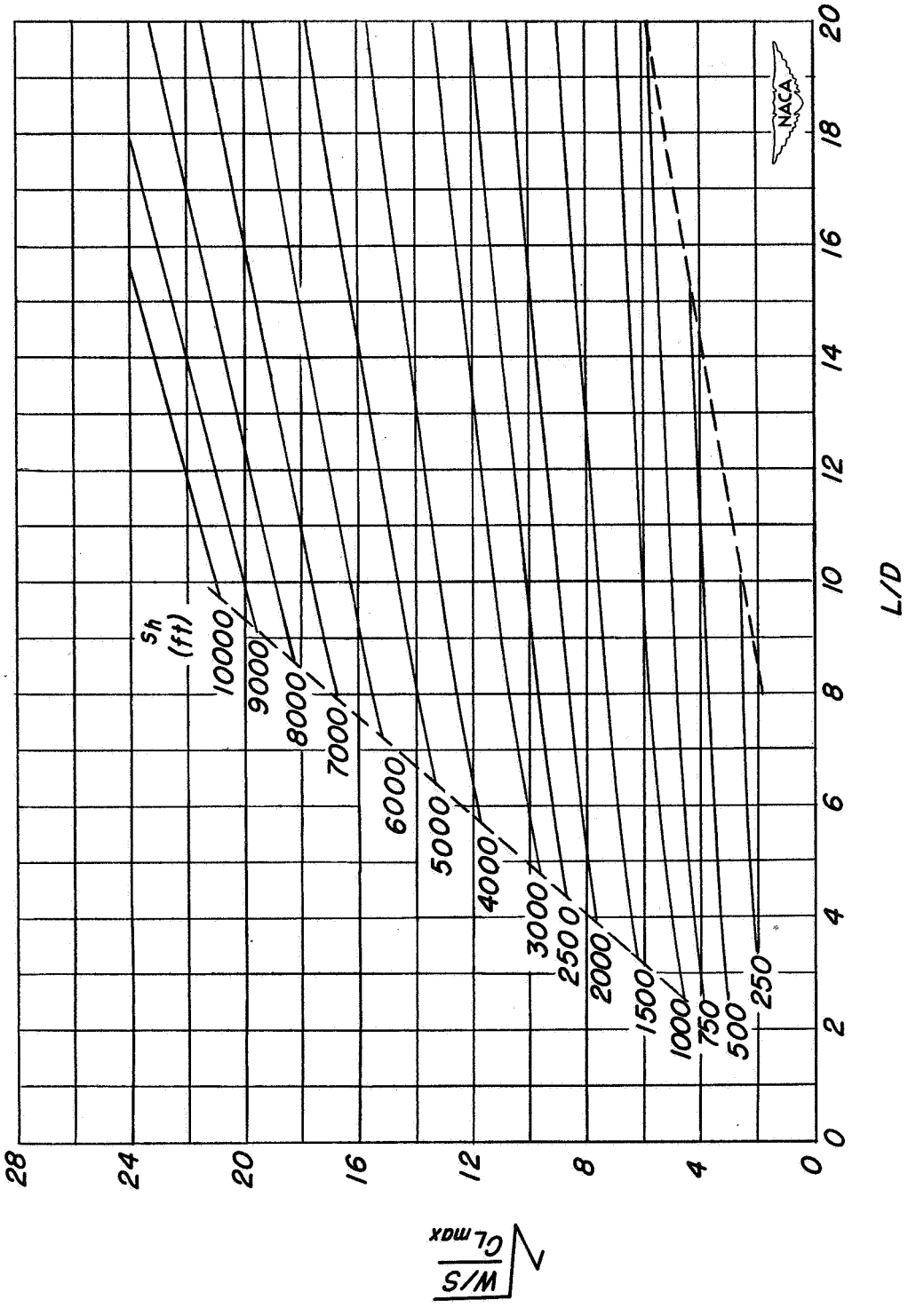

Figure 6.- Variation of horizontal distance s_h required for the landing flare with L/D and $\sqrt{W/S}_{C_{L_{max}}}$.

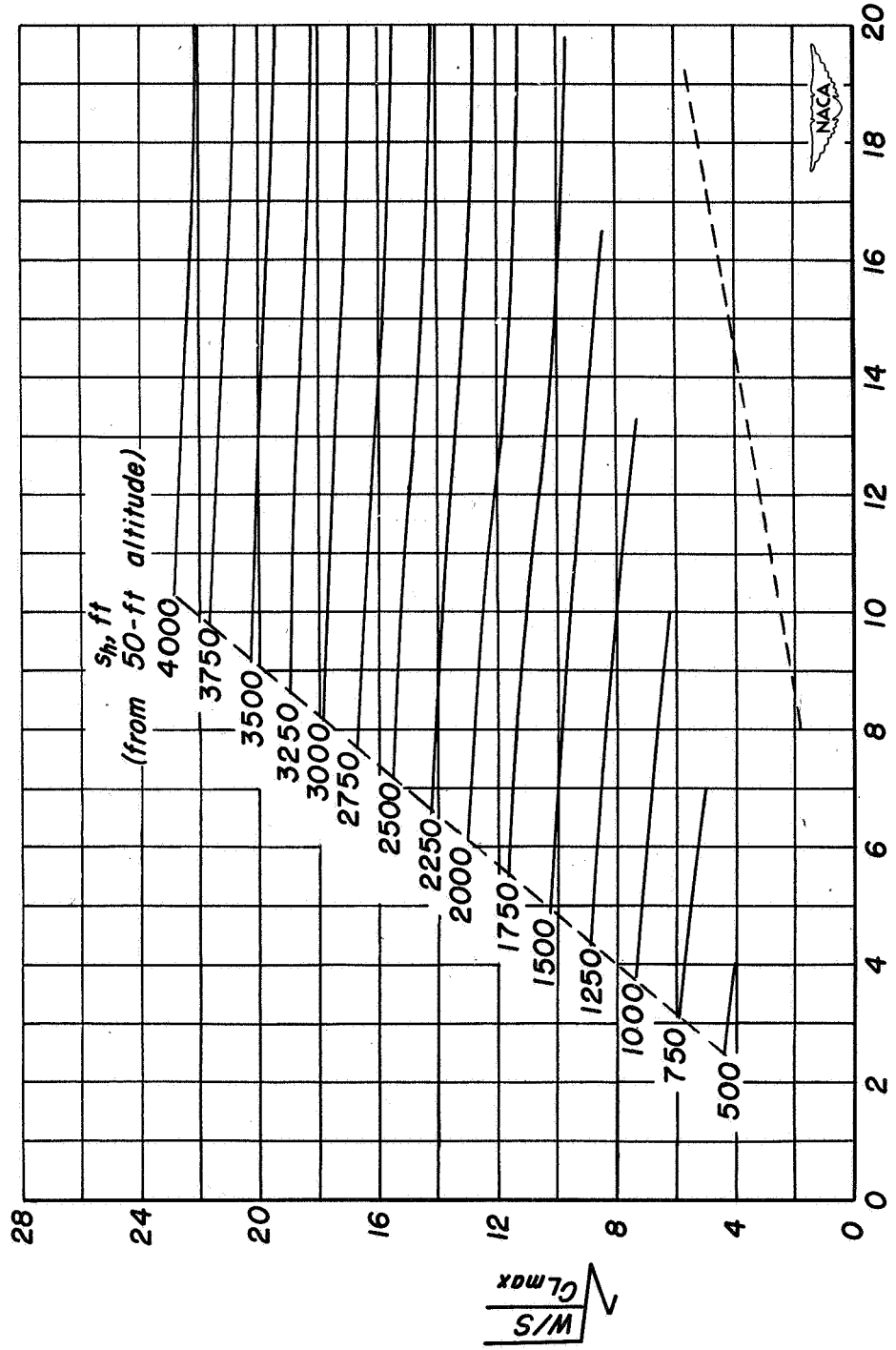

Figure 7.- Variation of horizontal distance s_h required from an altitude of 50 feet to the end of the landing flare with L/D and $\sqrt{\frac{W/S}{C_{L_{max}}}}$.

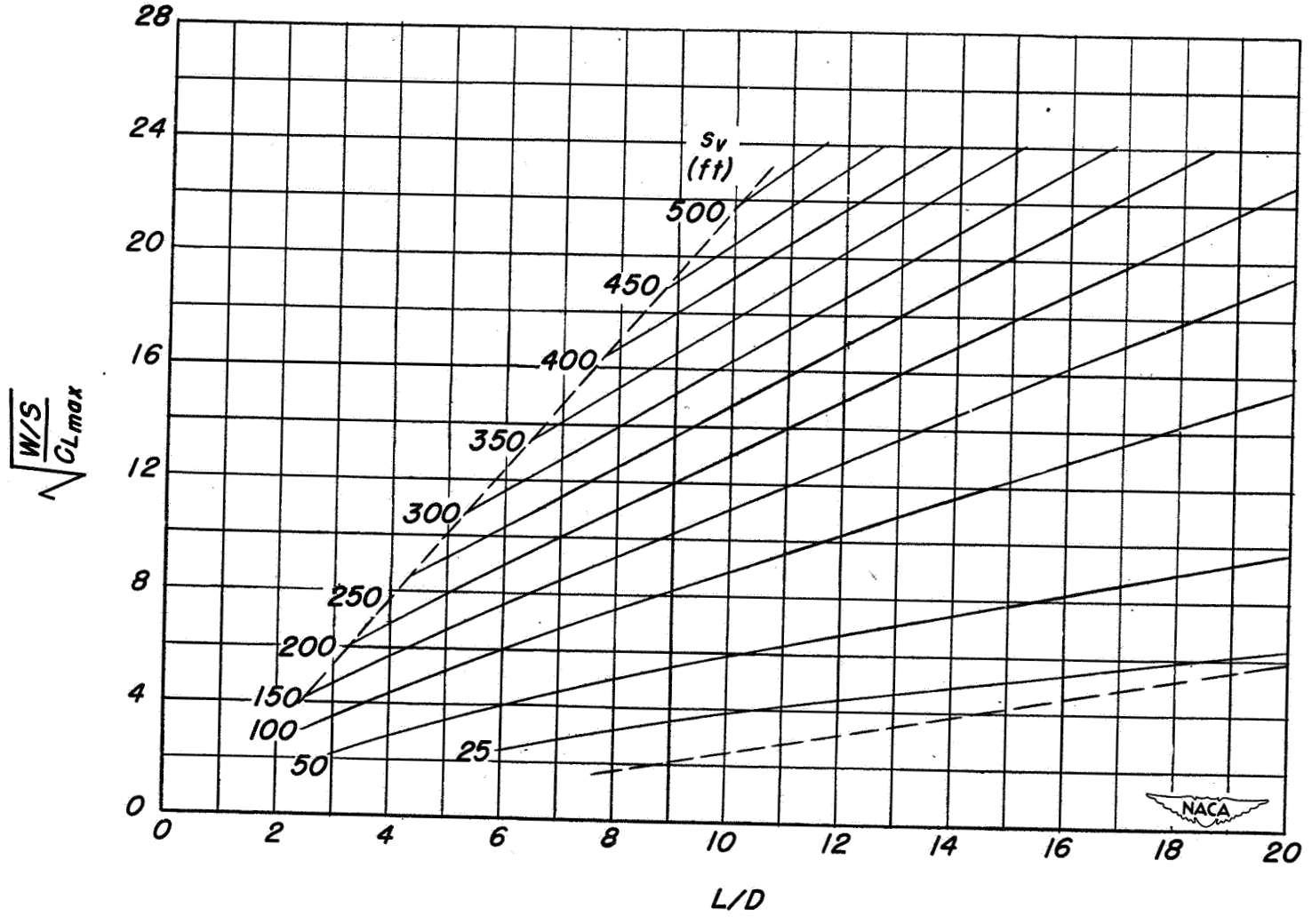

Figure 8.– Variation of vertical distance s_v required for the landing flare with L/D and $\sqrt{\frac{W/S}{C_{L_{max}}}}$.

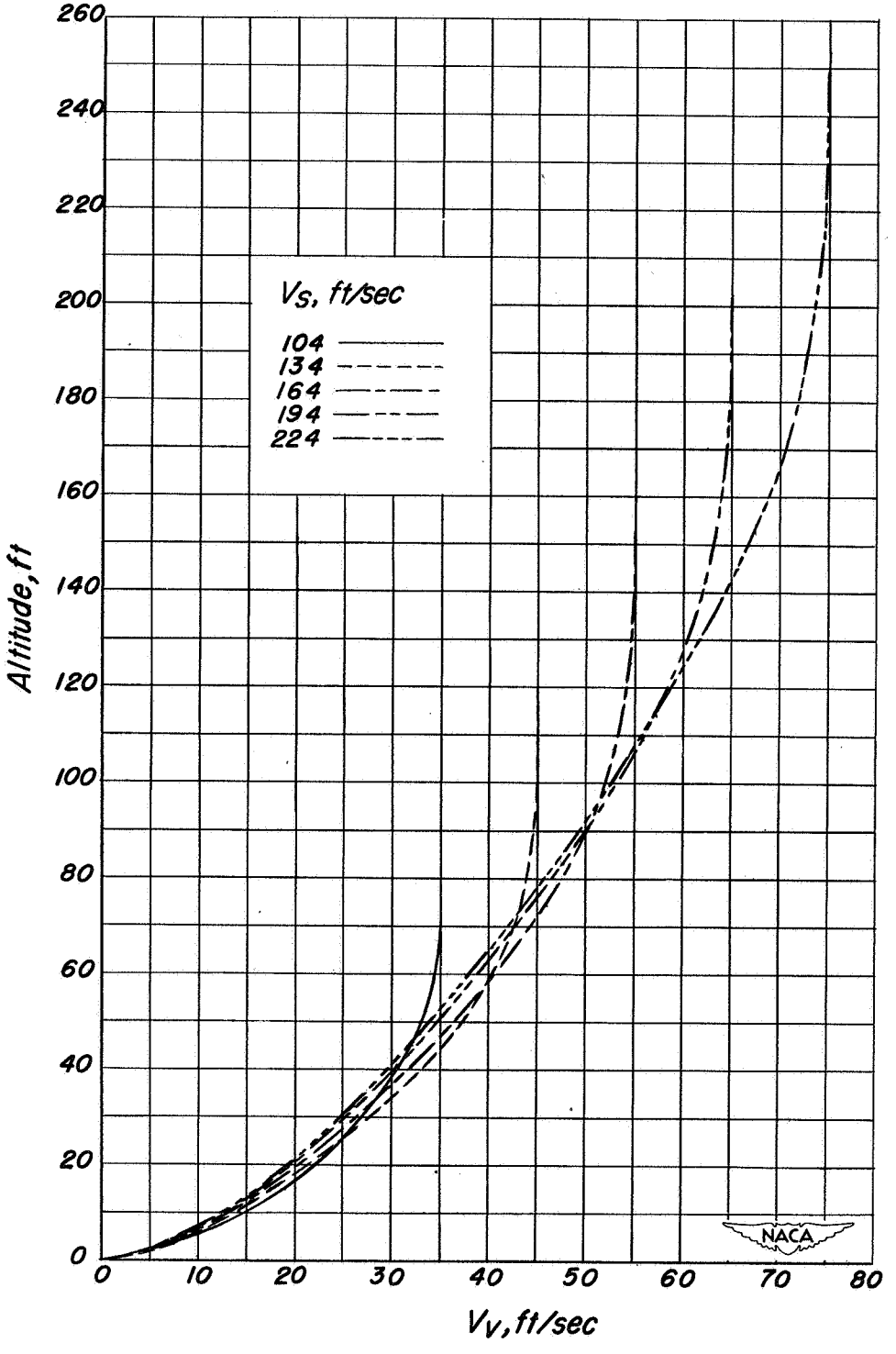

(a) $\frac{L}{D} = 4.$

Figure 9.– Variation of sinking speed in the landing flare with altitude for several stalling speeds.

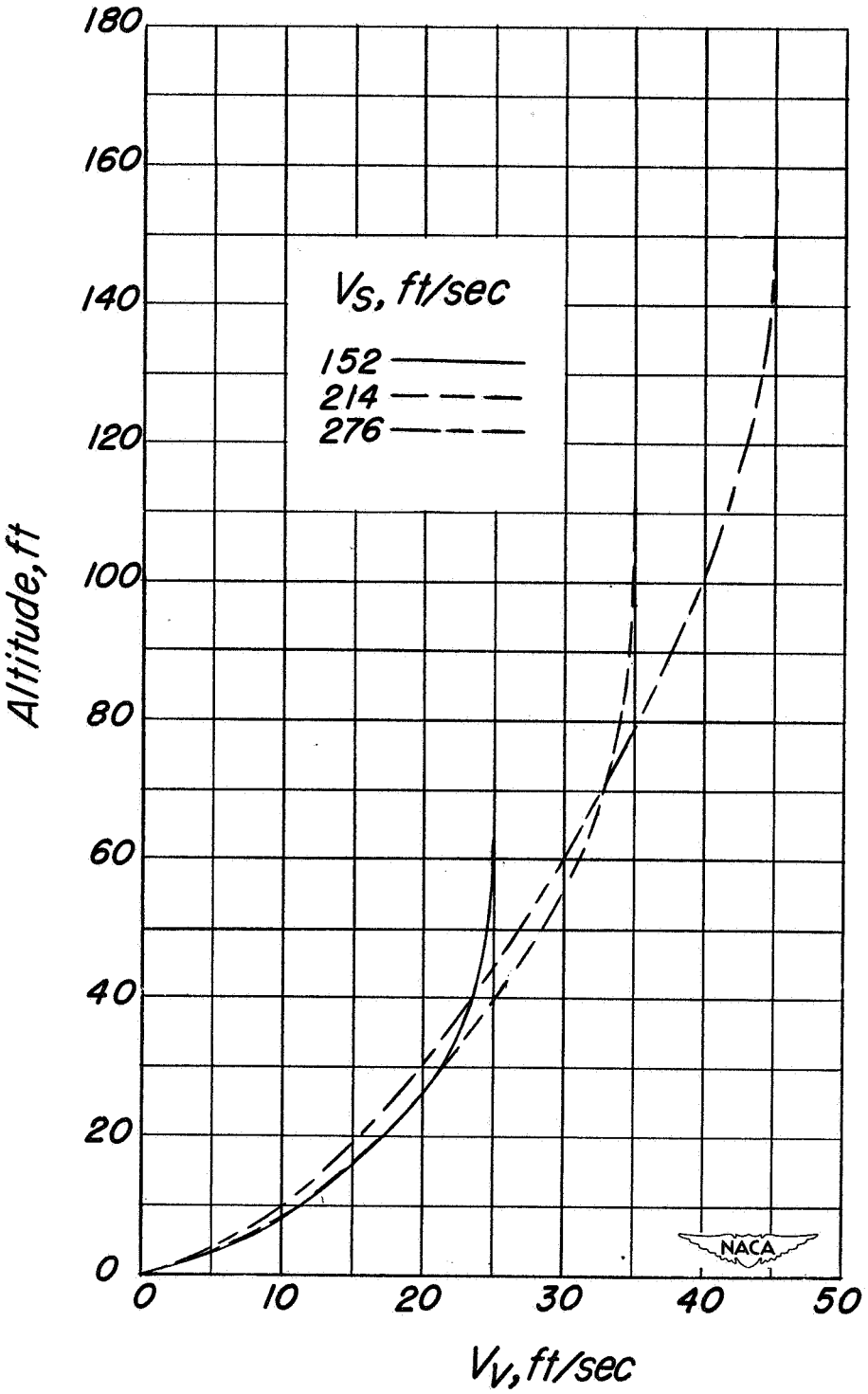

(b) $\frac{L}{D} = 7.5$.

Figure 9.– Concluded.

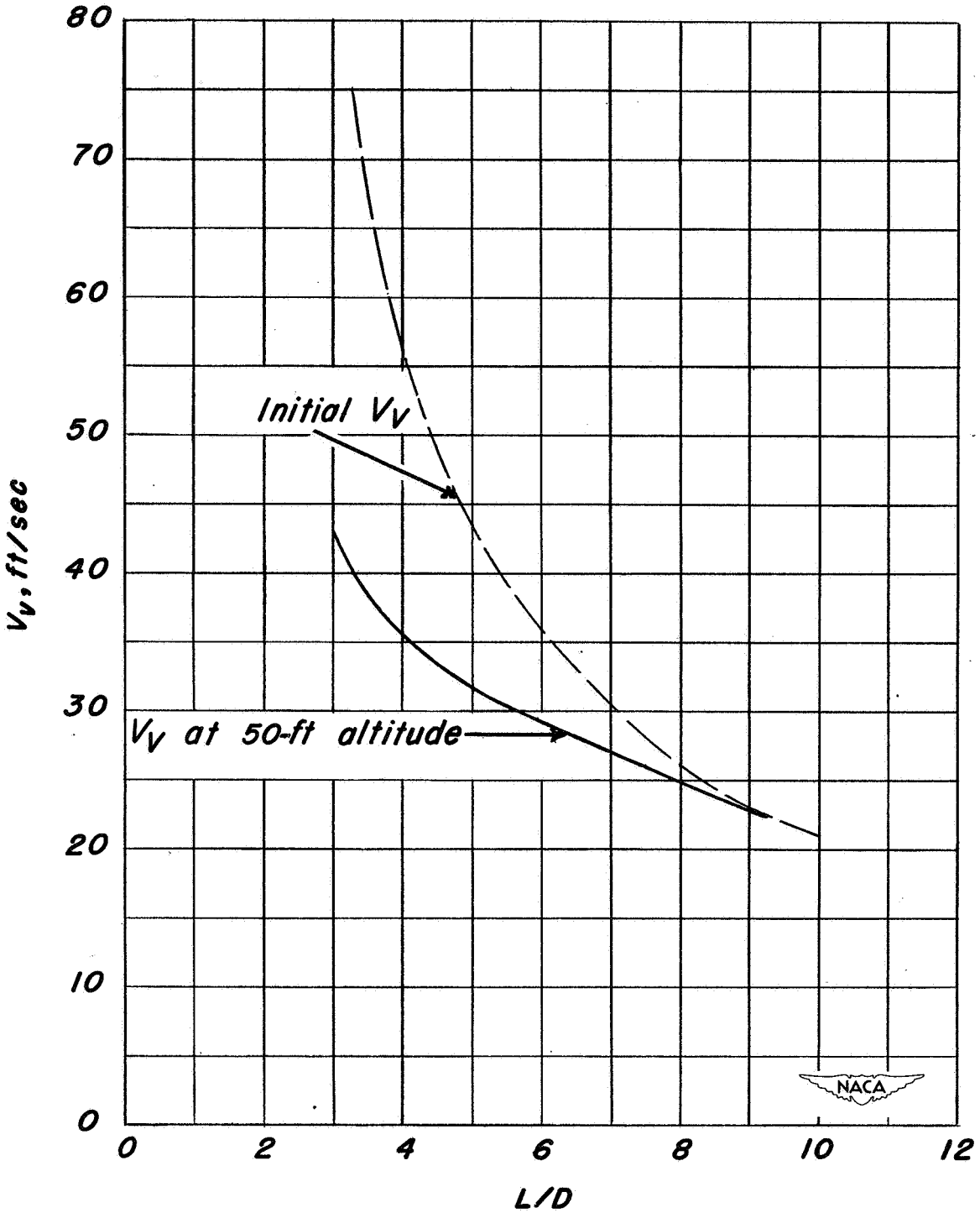

Figure 10.- Variation with L/D of the initial sinking speed and the sinking speed at an altitude of 50 feet for a stalling speed of 167 feet per second. $\frac{W}{S}$ = 40 pounds per square foot; $C_{L_{max}}$ = 1.2.

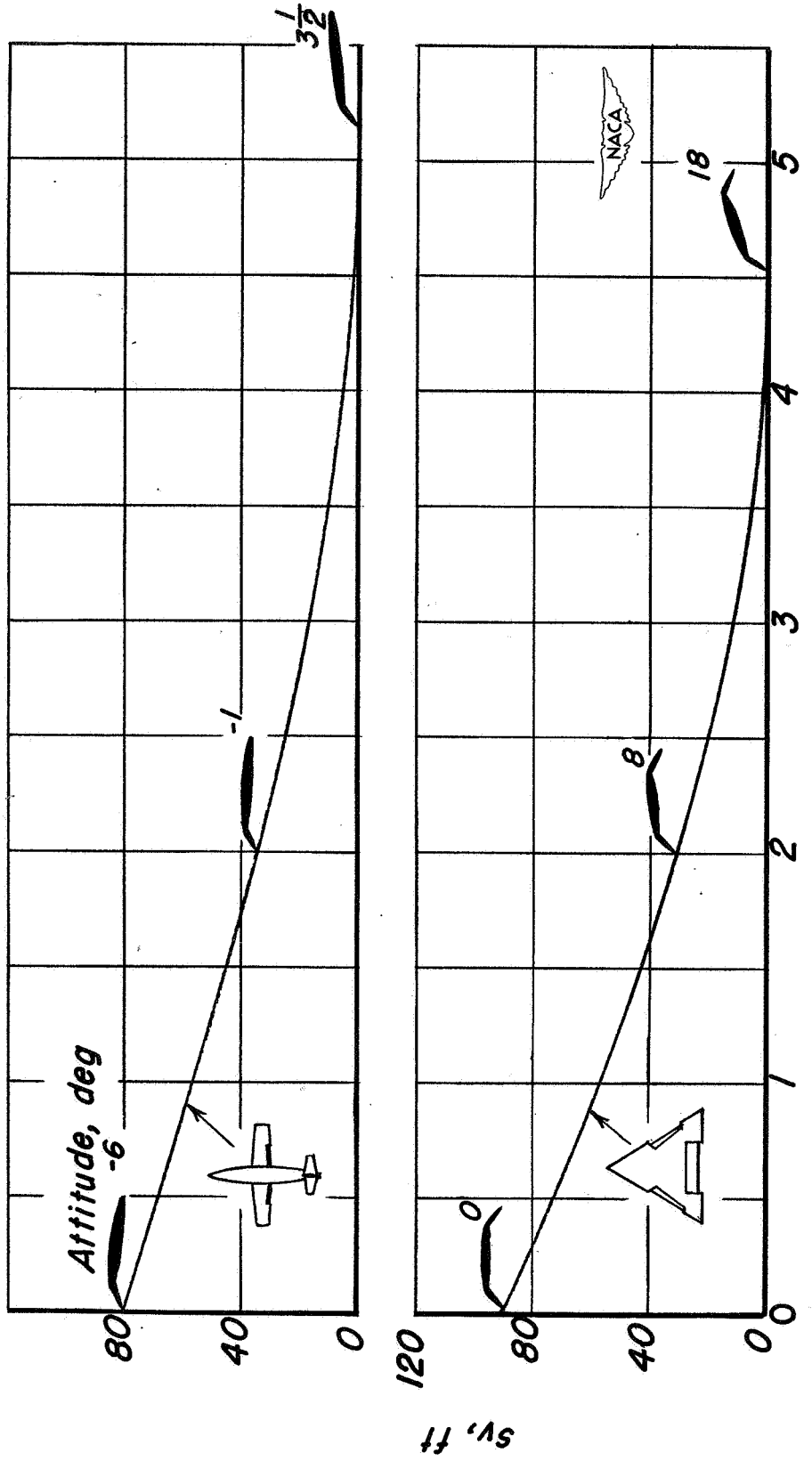

Figure 11.- Attitude variations during power-off landing flares of a triangular wing with flaps and of airplane C of figure 1. $\frac{W}{S}$ = 40 pounds per square foot.

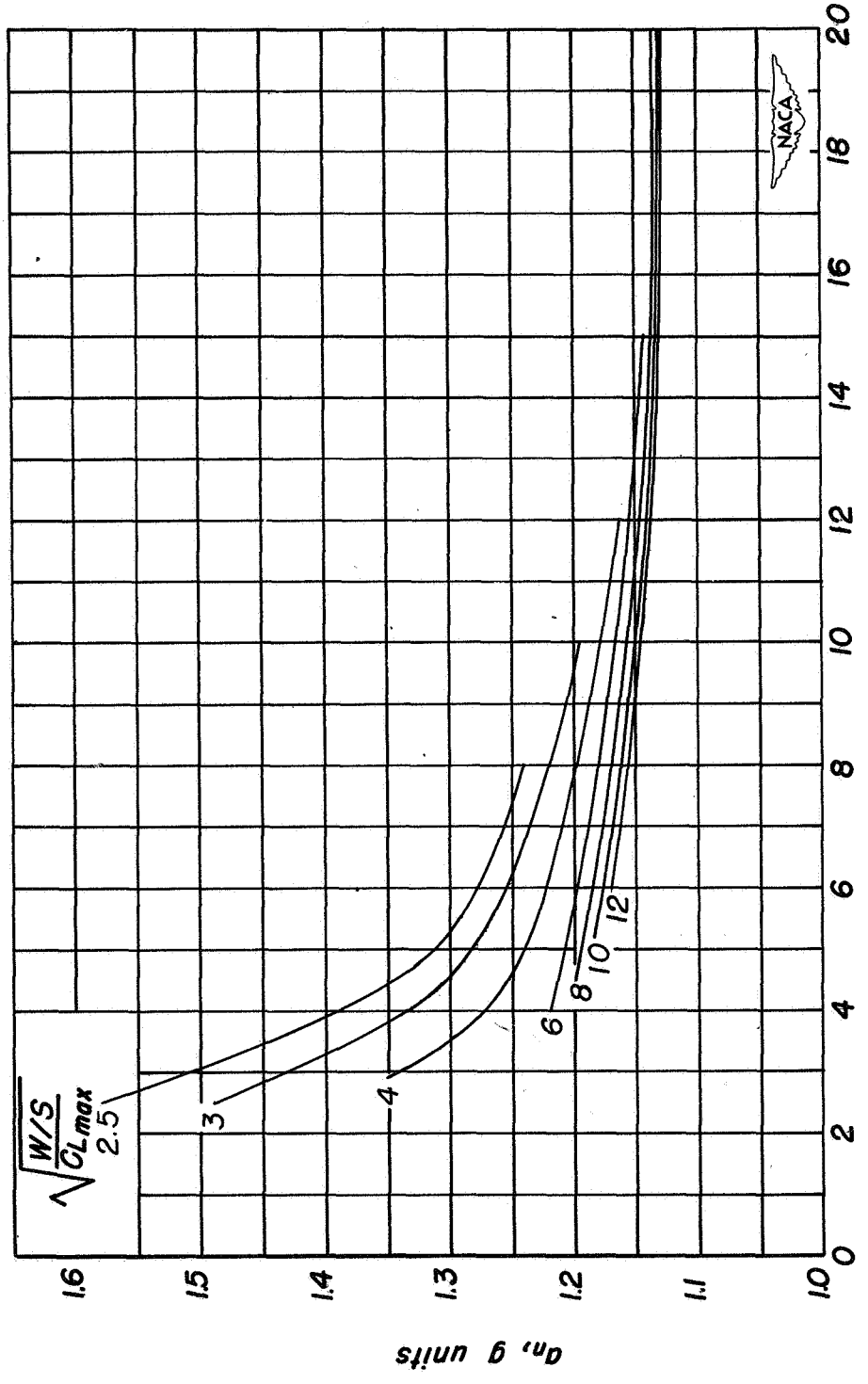

Figure 13.- Variation of the normal acceleration 1 second prior to the end of the flare with L/D and $\sqrt{\frac{W/S}{C_{L_{max}}}}$.